

Hybrid Beamforming Analysis Based on MIMO Channel Measurements at 28 GHz

Joerg Eisenbeis*, Magnus Tingulstad, Nicolai Kern, Zsolt Kollár, Jerzy Kowalewski,
Pablo Ramos López, and Thomas Zwick

Institute of Radio Frequency Engineering and Electronics (IHE),
Karlsruhe Institute of Technology (KIT), Germany

*joerg.eisenbeis@kit.edu

Abstract—Hybrid beamforming systems represent an efficient architectural solution to realize massive multiple-input multiple-output (MIMO) communication systems in the centimeter wave (cmW) and millimeter wave (mmW) region. These hybrid beamforming systems separate the beamforming process into a digital and analog beamforming network. The analog beamforming networks can be realized by different architectural solutions, which demand dedicated algorithms to determine the complex weighting factors in the digital and analog domain. To date, novel hybrid beamforming architectures and algorithms are solely compared in numerical simulations based on statistical channel models. These abstract channel models simplify the complicated electromagnetic propagation process, thereby not exactly reconstructing the wireless channel. Within this work, we present a measurement-based evaluation of hybrid beamforming algorithms and compare them with numerical results gained from a statistical path-based MIMO channel model. The results show that by adjustment of the channel model parameter the simulation achieves a good match with the measured maximum achievable spectral efficiencies.

Index Terms—MIMO, Millimeter wave radio communication, Mobile communication, Beam steering

I. INTRODUCTION

To meet the demand of higher data rates in mobile communication networks massive MIMO systems are proposed operating in the cmW and mmW region. For this purpose the 3rd Generation Partnership Project (3GPP) lately defined the *n257*-band between 26.5 GHz - 29.5 GHz [1]. As the number of spatial propagation paths is limited at higher frequencies, due to higher path loss coefficients [2], the number of digital channels can be adjusted with respect to the propagation scenario and frequency band. To preserve a precise beamforming towards the users to overcome the severe path loss, the system may be expanded by an analog beamforming network located between the digital channels and the antenna elements [3]. This so-called hybrid beamforming approach shifts the demand of a precise beam steering partly in the analog domain, where mostly phase shifters are used [4], [5]. This reduces the number of digital channels compared to fully digital MIMO systems significantly. Nevertheless, due to the reduced beamforming flexibility and architectural constraints of the analog network, a loss in achievable spectral efficiency has to be taken into account [3].

The proposed hybrid beamforming architectures and algorithms in literature are mostly analyzed in numerical simu-

lations using statistical models of the wireless propagation channel. These models are commonly extended versions of the Saleh-Valenzuela model as presented in [6]–[10]. These statistical models generate random snapshots of the complex MIMO channel matrix, but depend on simplifications of the complex wireless propagation effects. To determine the achievable spectral efficiency and compare the hybrid beamforming architectures and algorithms in real mobile wireless propagation scenarios, outdoor measurements have to be performed.

This work focuses on analyzing the subarray-based hybrid beamforming architecture (also denominated in literature as *sub-connected* or *partially-connected* hybrid beamforming architecture) using outdoor measurements presented by the authors in [11]. Three algorithms for calculating the complex weighting factors of the analog beamforming network are compared, among them a simple algorithm based on the angular information of the spatial propagation paths. The results reveal the achievable maximum spectral efficiency of different beamforming algorithms using measured subsequent snapshots of the complex narrow-band MIMO channel matrix in typical small cell uplink mobile communication scenarios. Furthermore, the measurement-based results are compared with numerical simulations using a statistical path-based MIMO channel model.

II. SUBARRAY-BASED HYBRID BEAMFORMING ARCHITECTURE AND ALGORITHMS

In general, the beamforming matrix of a hybrid beamforming system $\mathbf{B} = \mathbf{B}_{\text{RF}} \cdot \mathbf{B}_{\text{BB}}$ is divided into a digital beamforming matrix $\mathbf{B}_{\text{BB}} \in \mathbb{C}^{N_{\text{dig}} \times N_{\text{bf}}}$ and an analog beamforming matrix $\mathbf{B}_{\text{RF}} \in \mathbb{C}^{N_{\text{ant}} \times N_{\text{dig}}}$. Thereby, N_{ant} is the number of antenna elements, N_{dig} is defined as the number of digital channels and N_{bf} accounts for the number of parallel data streams transmitted assuming spatial multiplexing transmission technique [12]. The goal of the hybrid beamforming algorithms is to maximize the spectral efficiency under the constraints of the hybrid beamforming architecture, meaning the analog beamforming network [3]. Furthermore, the limited resolution of the phase shifters, additional component losses and the possibility of absence of amplitude weighting in the analog beamforming networks have to be taken into account.

Within this work, we focus on subarray-based hybrid beamforming systems, which are characterized by the low-

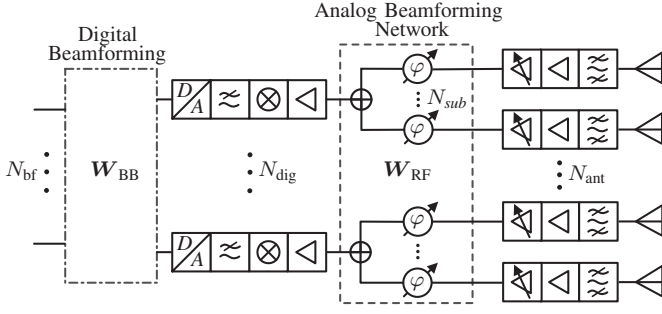


Fig. 1. Block diagram of an exemplary subarray-based hybrid beamforming Rx architecture.

complex circuitry design of the analog beamforming network and consequently efficient and cheap implementation. The analog beamforming network of the subarray-based hybrid beamforming architecture connects each digital channel with an independent subarray of antennas as shown for the receiver (Rx) in Fig. 1. In front of each antenna a phase shifter is placed to achieve a precise beam steering. As a result the required number of phase shifters is equal to the number of antenna elements. Due to the architectural constraints the analog beamforming matrix at the Rx [8]

$$\mathbf{B}_{\text{RF}} = \begin{bmatrix} \vec{v}_1 & 0 & \cdots & 0 \\ 0 & \vec{v}_2 & & 0 \\ \vdots & & \ddots & \vdots \\ 0 & 0 & 0 & \vec{v}_{N_{\text{bf}}} \end{bmatrix} \quad (1)$$

is of block-diagonal form containing the $N_{\text{bf}} \leq \min\{M_{\text{dig}}, N_{\text{dig}}\}$ beamforming vectors of size $\vec{v}_m \in \mathbb{C}^{N_{\text{sub}} \times 1}$, $\forall m = \{1, 2, \dots, N_{\text{bf}}\}$. Thereby $N_{\text{sub}} = N_{\text{ant}}/N_{\text{dig}}$ denotes the number of antennas per subarray. As no amplitude weighting in the analog domain is performed, the amplitudes of all coefficients are equal. To satisfy the overall power constraint, the Frobenius norm of the combined beamforming matrix satisfies $\|\mathbf{B}_{\text{RF}} \cdot \mathbf{B}_{\text{BB}}\|_F^2 = N_{\text{dig}}$.

One approach to determine the analog beamforming matrix is the successive interference cancellation (SIC)-based hybrid beamforming algorithm presented by Gao et al. in [8]. The algorithm aims to maximize the total achievable data rate by dividing the non-convex optimization problem into a sub-rate optimization for each subarray. Thereby each subarray is seeking a beamforming vector which minimizes the Euclidean distance to the optimal unconstrained solution [8]. To account for the limited phase shifter resolution q the calculated beamforming coefficients are subsequently adjusted to fulfill this constraint. Furthermore, the authors in [8] presented a processing optimized approach by replacing the required matrix inversion with a numerical approximation.

Note that the algorithms presented in [8] require the full MIMO channel matrix as input, which might be challenging and time-consuming to obtain due to the constraints within the analog beamforming network. Moreover, current research on hybrid beamforming channel estimation algorithms focuses on estimating the angles of departure and arrival to identify the

spatial propagation paths for the subsequent beamforming process [13]–[17]. Therefore, we construct a codebook-based algorithm for subarray-based hybrid beamforming systems only requiring knowledge about the angles of departure (AoDs) at the transmitter (Tx) and angles of arrival (AoAs) at the Rx. Similar to [16], [17] a codebook is constructed for the uniform linear array using the array response vector

$$\vec{a}(\theta) = \frac{1}{\sqrt{N_{\text{sub}}}} \left[1, e^{j \frac{2\pi}{\lambda_0} d \sin(\theta)}, \dots, e^{j(N_{\text{sub}}-1) \frac{2\pi}{\lambda_0} d \sin(\theta)} \right] \quad (2)$$

where d represents the antenna spacing and θ the desired angle of arrival or departure. As the phase shifter resolution is limited in most practical realizations, the angular resolution of the effective beam

$$\Delta\theta = \arcsin \left\{ \frac{\lambda_0}{2\pi d} \cdot \Delta\vartheta \right\} \quad (3)$$

is restricted by the minimal step width of the phase shifter

$$\Delta\vartheta = 2\pi/2^q \quad (4)$$

with a resolution of q bit. Based on the resolution constraints, the possible angles for the constructed codebook are limited to $\theta = \{\dots, -2\Delta\theta, -\Delta\theta, 0, \Delta\theta, 2\Delta\theta, \dots\}$. To utilize spatial multiplexing technique we first estimate the strongest N_{bf} AoDs or AoAs within the channel sounding process denoted by $\vec{\xi} = [\xi_1, \xi_2, \dots, \xi_K]$. The N_{bf} beamforming vectors are selected by minimizing the euclidean distance between each estimate ξ and the possible predefined angles. The index of the k -th strongest AoA or AoD results to

$$\omega_k = \min_i \{|\vec{\theta}(i) - \xi_k|\} \quad (5)$$

and enables the construction of the analog beamforming matrix

$$\mathbf{B}_{\text{RF}} = \begin{bmatrix} \vec{a}(\vec{\theta}(\omega_1))^T & 0 & \cdots & 0 \\ 0 & \vec{a}(\vec{\theta}(\omega_2))^T & & 0 \\ \vdots & & \ddots & \vdots \\ 0 & 0 & 0 & \vec{a}(\vec{\theta}(\omega_K))^T \end{bmatrix} \quad (6)$$

based on the predefined array response vectors in eq. 2. It is thereby important to adjust the phase difference between the neighboring subarrays to optimize the beam pattern, which can be done in the digital domain by adjusting \mathbf{B}_{BB} .

III. MEASUREMENT DATA AND SPECTRAL EFFICIENCY

The outdoor measurements used are conducted in three small cell site scenarios with in total 159 different Tx locations emulating an uplink communication scenario between a mobile entity as Tx and a radio base station as Rx [11]. The measurements are performed between 4 Tx and 16 Rx antennas at a center frequency of 27.8 GHz. At the Tx four monopole antennas arranged in a square and separated by $0.55 \cdot \lambda$ are used, where λ represents the wavelength at 27.8 GHz. For the Rx a uniform linear array with 16 microstrip patch elements and an element spacing of $\lambda/2$ are employed. The MIMO measurement system is used to calculate subsequent narrow-band snapshots of the complex MIMO channel matrix for a

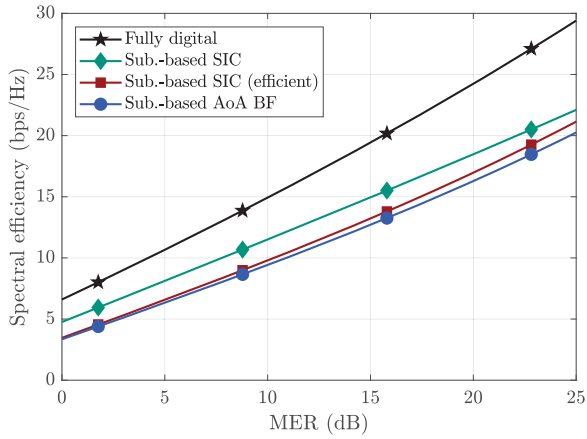


Fig. 2. Spectral efficiency over the MER for different subarray-based hybrid beamforming algorithms.

fixed location of the Tx and Rx. Furthermore, the calculated modulation error rate (MER) serves as an estimate of the signal-to-noise ratio (SNR). For each location a recording of around 20 s is made. A more detailed description of the measurement principle, setup and scenarios can be found in [11].

Due to the limited number of transmit antennas, the subarray-based hybrid beamforming architecture is only applied at the Rx side. At the mobile Tx a fully digital MIMO system is assumed. To analyze the performance of the different hybrid beamforming algorithms we calculate the spectral efficiency or maximum sum data rate [18]

$$R = \log_2 \left\{ \left| \mathbf{I}_{N_{\text{ant}}} + \frac{\gamma}{M_{\text{ant}}} \mathbf{W}^H \mathbf{H} \mathbf{F} \mathbf{F}^H \mathbf{H}^H \mathbf{W} \right| \right\}, \quad (7)$$

where γ denotes the SNR at the Rx, $\mathbf{I}_{N_{\text{ant}}}$ the identity matrix of dimension N_{ant} , $\mathbf{F} \in \mathbb{C}^{M_{\text{ant}} \times N_{\text{bf}}}$ the precoding matrix at the Tx and $\mathbf{W} = \mathbf{W}_{\text{RF}} \cdot \mathbf{W}_{\text{BB}} \in \mathbb{C}^{N_{\text{ant}} \times N_{\text{bf}}}$ the equalization matrix at the Rx.

IV. MEASUREMENT-BASED ANALYSIS

For the measurement-based analysis the number of digital channels is set equal to the number of parallel data streams to $N_{\text{dig}} = N_{\text{bf}} = 4$ leading to four subarrays, i.e. $N_{\text{sub}} = 4$. This means, that the Tx side remains fully digital, leading to $M_{\text{ant}} = M_{\text{dig}} = 4$ in all presented results. The resolution of the assumed digital phase shifters is $q = 6$ bit for the hybrid beamforming architecture.

In Fig. 2 the different subarray-based hybrid beamforming algorithms are compared. The spectral efficiency of the fully digital architecture serves as upper performance boundary. The results show that the subarray-based hybrid beamforming architecture suffers from a performance loss due to the reduced flexibility introduced by the analog beamforming network. This is consistent with the results presented in previous studies based on numerical analysis [8]. The proposed SIC-algorithm presented in [8] (designated as: *Sub.-based SIC*) achieves the highest spectral efficiency of the subarray-based hybrid

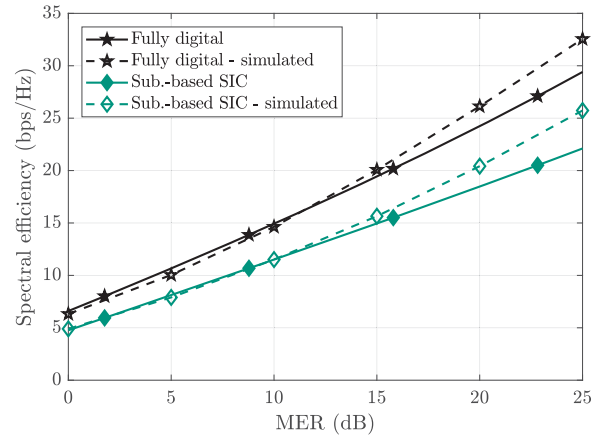


Fig. 3. Comparison of the spectral efficiency between the fitted curves based on the measurement data and the results gained from numerical analysis. For the numerical analysis the path-based MIMO channel model presented in [19] is employed, where the simulation parameters are adjusted to the findings obtained by channel measurements. The comparison is performed for the fully digital architecture and subarray-based hybrid beamforming architecture using the best performance algorithm presented in [8].

beamforming algorithms in our evaluation. The results show that the algorithm lies only around 4 bps/Hz below the fully digital approach at a channel MER of 10 dB. The processing optimized approach proposed in [8] (designated as: *Sub.-based SIC (efficient)*) visibly reduces the performance, here by 1.7 bps/Hz at a MER of 10 dB, compared to the best performing subarray-based hybrid beamforming algorithm. The algorithm based on the estimated AoAs remains only slightly below the efficient subarray-based hybrid beamforming algorithm presented in [8].

To validate the abstract channel models used for hybrid beamforming architecture and algorithm comparison in literature, the results are compared with numerical simulations. Therefore, we employ the statistical path-based MIMO channel model presented in [19] to generate random snapshots of the MIMO wireless propagation channel. For each channel SNR 1000 snapshots are generated. The simulation parameters are adjusted to the findings obtained by the channel measurements. The AoDs are limited in azimuth and elevation to 360° and 30° and the AoAs are limited in azimuth and elevation to 120° and 45° , respectively. Furthermore, the simulated 3D element characteristics of the antennas used within the measurements are included at the Tx and Rx side respectively. In addition, the cumulative distribution function (CDF) of the eigenvalues is approximated to the measured characteristic by adjusting the number of spatial paths. The measurement-based, compared to the numerical determined achievable spectral efficiency, is shown in Fig. 3 for the fully digital and best performance subarray-based hybrid beamforming algorithm. The results show that the measured and simulated spectral efficiency of the complex subarray-based hybrid beamforming algorithm match quite well at lower MERs. For MER values above 15 dB the numerical analysis shows for the fully digital and subarray-based hybrid beamforming approach a higher

increase in spectral efficiency, which cannot be observed from the measurements. This means that the simulation is overestimating the achievable spectral efficiency at this point. A reason for this is the high attenuation introduced within the propagation paths with one or more reflections. As the signal wavelength gets smaller structural features of the reflecting objects lead to a more diffuse scattering [20]. Moreover, studies showed that foliage losses increase drastically at higher frequencies. This leads to mostly line-of-sight (LOS) dominated propagation scenarios, which have large differences in the channel eigenvalues. This is in general not the ideal environment for spatial multiplexing techniques and limits the achievable spectral efficiency.

V. CONCLUSION

This work presents a measurement-based analysis of subarray-based hybrid beamforming algorithms and compares the results with values gained from numerical simulations utilizing a statistical path-based MIMO channel model. A simple beamforming algorithm is proposed based on estimates of the AoAs and AoDs of the wireless propagation channel. Moreover, the algorithm is compared with state-of-the-art beamforming algorithms showing nearly similar performance, while no estimation of the full MIMO channel matrix is required. The results reveal that the statistical channel model can predict the achievable spectral efficiency at low channel SNRs but may overestimate the performance in the higher SNR region. This is attributable to the LOS dominance within small cell communication scenarios.

ACKNOWLEDGMENT

This work was supported by the Electronic Components and Systems for European Leadership (ECSEL) joint undertaking funded under H2020-EU.2.1.1.7. in frame of the TARANTO project with ID 737454 and the German Federal Ministry of Education under grant number 16ESE0211.

REFERENCES

- [1] *Technical Specification Group Radio Access Network; New frequency range for NR (24.25–29.5 GHz) (Release 15)*, 3rd Generation Partnership Project (3GPP), jun 2018, v1.0.0 (2018-06).
- [2] T. S. Rappaport, G. R. MacCartney, M. K. Samimi, and S. Sun, “Wide-band millimeter-wave propagation measurements and channel models for future wireless communication system design,” *IEEE Transactions on Communications*, vol. 63, no. 9, pp. 3029–3056, 2015.
- [3] A. F. Molisch, V. V. Ratnam, S. Han, Z. Li, S. L. H. Nguyen, L. Li, and K. Haneda, “Hybrid Beamforming for Massive MIMO: A Survey,” *IEEE Communications Magazine*, vol. 55, no. 9, pp. 134–141, 2017.
- [4] R. Mendez-Rial, C. Rusu, A. Alkhateeb, N. Gonzalez-Prelcic, and R. W. Heath, “Channel estimation and hybrid combining for mmWave: Phase shifters or switches?” in *2015 Information Theory and Applications Workshop, ITA 2015 - Conference Proceedings*. IEEE, feb 2015, pp. 90–97.
- [5] S. Payami, M. Ghoraihi, M. Dianati, and M. Sellathurai, “Hybrid Beamforming with a Reduced Number of Phase Shifters for Massive MIMO Systems,” *IEEE Transactions on Vehicular Technology*, vol. 67, no. 6, pp. 4843–4851, 2018.
- [6] O. E. Ayach, R. W. Heath, S. Abu-Surra, S. Rajagopal, and Z. Pi, “The capacity optimality of beam steering in large millimeter wave MIMO systems,” *IEEE Workshop on Signal Processing Advances in Wireless Communications, SPAWC*, pp. 100–104, 2012.
- [7] A. Alkhateeb, G. Leus, and R. W. Heath, “Limited Feedback Hybrid Precoding for Multi-User Millimeter Wave Systems,” *IEEE Transactions on Wireless Communications*, vol. 14, no. 11, pp. 6481–6494, 2015.
- [8] X. Gao, L. Dai, S. Han, I. Chih-Lin, and R. W. Heath, “Energy-Efficient Hybrid Analog and Digital Precoding for MmWave MIMO Systems with Large Antenna Arrays,” *IEEE Journal on Selected Areas in Communications*, vol. 34, no. 4, pp. 998–1009, apr 2016.
- [9] D. Zhang, Y. Wang, X. Li, and W. Xiang, “Hybridly Connected Structure for Hybrid Beamforming in mmWave Massive MIMO Systems,” *IEEE Transactions on Communications*, vol. 66, no. 2, pp. 662–674, feb 2018.
- [10] J. Eisenbeis, M. Krause, T. Mahler, S. Scherr, and T. Zwick, “Path based MIMO channel model for hybrid beamforming architecture analysis,” in *2018 11th German Microwave Conference (GeMiC)*. IEEE, mar 2018, pp. 311–314.
- [11] J. Eisenbeis, M. Tingulstad, N. Kern, K. Zsolt, J. Kowalewski, P. Ramos López, and T. Zwick, “MIMO Uplink Communication Measurements in Small Cell Scenarios at 28 GHz,” 2020, *Manuscript submitted for publication*.
- [12] P. Wolniansky, G. Foschini, G. Golden, and R. Valenzuela, “V-BLAST: an architecture for realizing very high data rates over the rich-scattering wireless channel,” in *1998 URSI International Symposium on Signals, Systems, and Electronics. Conference Proceedings (Cat. No.98EX167)*. IEEE, 2002, pp. 295–300.
- [13] A. Alkhateeb, O. El Ayach, G. Leus, and R. W. Heath, “Channel estimation and hybrid precoding for millimeter wave cellular systems,” *IEEE Journal on Selected Topics in Signal Processing*, vol. 8, no. 5, pp. 831–846, oct 2014.
- [14] J. Singh and S. Ramakrishna, “On the feasibility of codebook-based beamforming in millimeter wave systems with multiple antenna arrays,” *IEEE Transactions on Wireless Communications*, vol. 14, no. 5, pp. 2670–2683, 2015.
- [15] M. Kokshoorn, H. Chen, P. Wang, Y. Li, and B. Vucetic, “Millimeter Wave MIMO Channel Estimation Using Overlapped Beam Patterns and Rate Adaptation,” *IEEE Transactions on Signal Processing*, vol. 65, no. 3, pp. 601–616, feb 2017.
- [16] C. Lin, G. Y. Li, and L. Wang, “Subarray-Based Coordinated Beamforming Training for mmWave and Sub-THz Communications,” *IEEE Journal on Selected Areas in Communications*, vol. 35, no. 9, pp. 2115–2126, sep 2017.
- [17] Y. Zhu, Q. Zhang, and T. Yang, “Low-Complexity Hybrid Precoding With Dynamic Beam Assignment in mmWave OFDM Systems,” *IEEE Transactions on Vehicular Technology*, vol. 67, no. 4, pp. 3685–3689, apr 2018.
- [18] O. E. Ayach, S. Rajagopal, S. Abu-Surra, Z. Pi, and R. W. Heath, “Spatially Sparse Precoding in Millimeter Wave MIMO Systems,” *IEEE Transactions on Wireless Communications*, vol. 13, no. 3, pp. 1499–1513, mar 2014.
- [19] J. Eisenbeis, T. Mahler, P. Ramos López, and T. Zwick, “Channel Estimation Method for Subarray Based Hybrid Beamforming Systems Employing Sparse Arrays,” *Progress In Electromagnetics Research C*, vol. 87, no. August, pp. 25–38, 2018.
- [20] I. A. Hemadeh, K. Satyanarayana, M. El-Hajjar, and L. Hanzo, “Millimeter-Wave Communications: Physical Channel Models, Design Considerations, Antenna Constructions, and Link-Budget,” *IEEE Communications Surveys and Tutorials*, vol. 20, no. 2, pp. 870–913, 2018.